Advances in Applied Mathematics and Mechanics
Adv. Appl. Math. Mech., Vol. **10**, No. 1, pp. 184-208

DOI: 10.4208/aamm.2015.m1298
February 2018

Size-Dependent Geometrically Nonlinear Free Vibration of First-Order Shear Deformable Piezoelectric-Piezomagnetic Nanobeams Using the Nonlocal Theory

Raheb Gholami[1,*] and Reza Ansari[2]

[1] *Department of Mechanical Engineering, Lahijan Branch, Islamic Azad University, P.O. Box 1616, Lahijan, Iran*
[2] *Department of Mechanical Engineering, University of Guilan, P.O. Box 3756, Rasht, Iran*

Received 18 September 2015; Accepted (in revised version) 25 May 2017

Abstract. This article investigates the geometrically nonlinear free vibration of piezoelectric-piezomagnetic nanobeams subjected to magneto-electro-thermal loading taking into account size effect using the nonlocal elasticity theory. To this end, the size-dependent nonlinear governing equations of motion and corresponding boundary conditions are derived according to the nonlocal elasticity theory and the first-order shear deformation theory with von Kármán-type of kinematic nonlinearity. The effects of size-dependence, shear deformations, rotary inertia, piezoelectric-piezomagnetic coupling, thermal environment and geometrical nonlinearity are taken into account. The generalized differential quadrature (GDQ) method in conjunction with the numerical Galerkin method, periodic time differential operators and pseudo arc-length continuation method is utilized to compute the nonlinear frequency response of piezoelectric-piezomagnetic nanobeams. The influences of various parameters such as non-dimensional nonlocal parameter, temperature change, initial applied electric voltage, initial applied magnetic potential, length-to-thickness ratio and different boundary conditions on the geometrically nonlinear free vibration characteristics of piezoelectric-piezomagnetic nanobeams are demonstrated by numerical examples. It is illustrated that the hardening spring effect increases with increasing the non-dimensional nonlocal parameter, positive initial applied voltage, negative initial applied magnetic potential, temperature rise and decreases with increasing the negative initial applied voltage, positive initial applied magnetic potential and length-to-thickness ratio.

AMS subject classifications: 35XX, 65XX, 74XX

Key words: Piezoelectric-piezomagnetic nanobeams, geometrically nonlinear free vibration, nonlocal elasticity theory, size effect, magneto-electro-thermal loading.

*Corresponding author.
Emails: gholami_r@liau.ac.ir (R. Gholami), r_ansari@guilan.ac.ir (R. Ansari)

1 Introduction

Nanostructured elements such as nanobeams, nanoplates and nanoshells have been widely used as main components in nano- and micro-electro-mechanical systems (NEMS and MEMS). Especially, nano-sized structures made of the piezoelectric-piezomagnetic materials have attracted a great deal of attention in many research interests due to their outstanding inherent magneto-electro-thermo-mechanical coupling effects [1–6]. As the typical component in the NEMS and MEMS, piezoelectric-piezomagnetic nanobeams, nanoplates and nanoshells have a wide range of applications in nano actuators, transducers, resonators and robotics [7–12]. Hence, understanding the linear and nonlinear static and dynamic mechanical behaviors of piezoelectric-piezomagnetic nanostructures is essential for their applications. The investigation of geometrically nonlinear free vibration of piezoelectric-piezomagnetic nanostructures in the thermal environment is a major topic of current interest, which is utilized to fully realize the dynamic characteristic of piezoelectric-piezomagnetic nanostructures in the large amplitude vibrations.

There are some typical experiments such as nano/micro-bend test, nano/micro-torsion test and micro/nano indentation test [13–19] and atomistic simulations [20–22], which have reported the size-dependent mechanical characteristics of small-scale structures. Hence, it is of great signicance to consider the size effect in mechanical characteristics of piezoelectric-piezomagnetic nanostructures. Since the molecular dynamics simulations for large-scale nanostructures are restricted by computational capacities and conducting controlled experiments and operating precision at the nanoscale are difcult, the size-dependent continuum theories including the nonlocal elasticity theory [23], strain gradient elasticity theory [24], modified couple stress theory [25], modified strain gradient theory [26] and surface stress elasticity theory [27, 28] have been proposed and have been widely utilized to develop the size-dependent beam, plate and shell models for the analysis of size-dependent mechanical characteristics of these small-scale structures [29–37]. Among these theories, the Eringen's nonlocal elasticity theory is commonly utilized to develop the nonlocal continuum models in which the effect of small scale parameter is incorporated.

Recently, several studies have been performed to study the size-dependent static and dynamic behaviors of nanostructures based on the nonlocal elasticity theory. More recently, the nonlocal theory has been extended to investigate the size-dependent mechanical behaviors of the piezoelectric-piezomagnetic nano-scale structures. Ke and his co-authors studied the size-dependent thermoelectric-mechanical free vibration [38], geometrically nonlinear free vibration characteristics [39] and buckling and postbuckling [40] of piezoelectric nanobeams by means of the proposed linear and nonlinear Timoshenko beam models and nonlocal elasticity theory. Moreover, Ke et al. [41, 42] performed a series of studies to investigate the thermo-electro-mechanical vibration of piezoelectric nanoplates using the classical and first-order shear deformable plate theories. Asemi et al. [43] examined the geometrically nonlinear free vibration of piezoelectric nanoelectromechanical resonators. In another work, a nonlocal Love thin shell model

was proposed by Ke et al. [44] to analyze the free vibration of piezoelectric cylindrical nanoshells under various edge supports. Moreover, a few studies have been performed on the piezoelectric-piezomagnetic nanostructures including nanobeams, nanoplates and nanoshells by means of nonlocal elasticity theory. Ke and Wang [45] examined the influence of the size effect, electric voltage and magnetic potential on the free vibration of a piezoelectric-piezomagnetic Timoshenko nanobeam. Ansari and Gholami [46] numerically investigated the free vibration characteristics of piezoelectric-piezomagnetic rectangular nanoplates with various boundary condition in the pre- and post-buckled states. Recently, Ke et al. [47, 48] analyzed the size-dependent free vibration of piezoelectric-piezomagnetic nanoplates and embedded nanoshells subjected to the magneto-electro-thermo-mechanical loading.

Unlike nanostructures made of piezoelectric materials, the mechanical behaviors of nanostructures made of piezoelectric-piezomagnetic materials have not been extensively explored. Specifically, to the best of authors' knowledge, the size-dependent geometrically nonlinear free vibration characteristics of first-order shear deformable piezoelectric-piezomagnetic nanobeams with different boundary conditions and under magneto-electro-thermal loading have not been studied so far. In this regard, this study is intended to analyze the size-dependent geometrically nonlinear free vibration of the piezoelectric-piezomagnetic nanobeams by means of the nonlocal elasticity theory and von Kármán geometric nonlinearity. The nonlocal piezoelectric-piezomagnetic nanobeam model is developed based on the first-order shear deformation beam theory. The influences of small-scale effect, magneto-electro-thermal coupling effect, transverse shear deformation and rotary inertia are taken into account. The nonlinear partial differential governing equations of motion and corresponding boundary conditions are discretized using the generalized differential quadrature (GDQ) method. Afterwards, the numerical Galerkin method and the periodic time differential operators together with pseudo arc-length continuation scheme are conducted to obtain the nonlinear frequency-amplitude response curves associated with the geometrically nonlinear free vibration of the piezoelectric-piezomagnetic nanobeams with various edge supports. The effects of non-dimensional nonlocal parameter, temperature change, initial applied electric voltage, initial applied magnetic potential, length-to-thickness ratio and end supports on the nonlinear free vibration characteristics of piezoelectric-piezomagnetic nanobeams are investigated through various numerical examples.

2 Nonlocal theory for the piezoelectric-piezomagnetic elastic materials

As mentioned in Section 1, the nonlocal elasticity theory emerged from the Eringen [49–51], which could potentially play an important role in the analysis of engineering problems related to nanotechnology applications, has been utilized in the mathematical formulation and mechanical analysis of nanostructures made of the piezoelectric-

piezomagnetic elastic materials. According to the theory of nonlocal elasticity, the equivalent differential forms of the nonlocal constitutive equations for the piezoelectric-piezomagnetic elastic materials can be expressed as

$$\sigma_{ij}-(e_0a)^2\nabla^2\sigma_{ij}=c_{ijkl}\varepsilon_{kl}-e_{mij}E_m-q_{nij}H_n-\beta_{ij}\Delta T, \tag{2.1a}$$

$$D_i-(e_0a)^2\nabla^2D_i=e_{ikl}\varepsilon_{kl}+s_{im}E_m+d_{in}H_n+p_i\Delta T, \tag{2.1b}$$

$$B_i-(e_0a)^2\nabla^2B_i=q_{ikl}\varepsilon_{kl}+d_{im}E_m+\mu_{in}H_n+\lambda_i\Delta T, \tag{2.1c}$$

in which ε_{ij}, E_i, B_i, H_i, denote the components of stress tensor, strain tensor, electric displacement vector, electric field vector, magnetic induction vector and magnetic field vector, respectively. Moreover, Φ, Ψ, c_{ijkl}, e_{mij}, s_{im}, q_{ij}, d_{ij}, μ_{ij}, p_i, λ_i, denote the elastic, piezoelectric, dielectric constants, piezomagnetic, magnetoelectric, magnetic, pyroelectric and pyromagnetic material properties, respectively; the thermal moduli and temperature change are represented by β_{ij}, ΔT, ∇^2, e_0a, is the nonlocal parameter.

3 Nonlocal geometrically nonlinear piezoelectric-piezomagnetic nanobeam model

A first-order shear deformable piezoelectric-piezomagnetic nanobeam with length L, thickness h, area of cross section A and moment of inertia I subjected to thermo-electromagnetic loading is considered in the Cartesian coordinate system. Upon the first-order shear deformation beam theory, the displacement field of an arbitrary point in the piezoelectric-piezomagnetic nanobeam can be expressed as

$$u_x(t,x,z)=U(t,x)+z\Theta_x(t,x), \qquad u_z(t,x,z)=W(t,x), \tag{3.1}$$

where u_x and u_z are the displacements parallel to the x- and y- axes, respectively; U and W represent the axial and transverse displacements of a given point in the mid-plane, respectively; Θ_x denotes the rotation of beam cross-section with respect to y-axis and t is the time.

According to the von Kármán type geometrical nonlinearity, the non-zero components of strain tensor based on the aforementioned displacement field (3.1) can be written as:

$$\varepsilon_{xx}=\frac{\partial u_x}{\partial x}+\frac{1}{2}\left(\frac{\partial W}{\partial x}\right)^2=\frac{\partial U}{\partial x}+z\frac{\partial\Theta_x}{\partial x}+\frac{1}{2}\left(\frac{\partial W}{\partial x}\right)^2, \quad \gamma_{xz}=\left(\Theta_x+\frac{\partial W}{\partial x}\right). \tag{3.2}$$

Assuming e_0a to be equal to zero, Eq. (2.1) can be used to express the classical coupled constitutive relations for piezoelectric-piezomagnetic nanobeam under the hypothesis of

plane stress state as follows:

$$\sigma_{xx}=\tilde{c}_{11}\varepsilon_{xx}-\tilde{e}_{31}E_z-\tilde{q}_{31}H_z-\tilde{\beta}_1\Delta T, \tag{3.3a}$$
$$\sigma_{xz}=\tilde{c}_{44}\gamma_{xz}-\tilde{e}_{15}E_x-\tilde{q}_{15}H_x, \tag{3.3b}$$
$$D_x=\tilde{e}_{15}\gamma_{xz}+\tilde{s}_{11}E_x+\tilde{d}_{11}H_x, \tag{3.3c}$$
$$D_z=\tilde{e}_{31}\varepsilon_{xx}+\tilde{s}_{33}E_z+\tilde{d}_{33}H_z+\tilde{p}_3\Delta T, \tag{3.3d}$$
$$B_x=\tilde{q}_{15}\gamma_{xz}+\tilde{d}_{11}E_x+\tilde{\mu}_{11}H_x, \tag{3.3e}$$
$$B_z=\tilde{q}_{31}\varepsilon_{xx}+\tilde{d}_{33}E_z+\tilde{\mu}_{33}H_z+\tilde{\lambda}_3\Delta T, \tag{3.3f}$$

in which the parameters $\tilde{c}_{ij}$, e_{ij}, $\tilde{q}_{ij}$ and $\tilde{s}_{ij}$ appeared in Eq. (3.3) are the reduced elastic, piezoelectric, piezomagnetic and magneto-electric constants, respectively. Also, $\tilde{d}_{ij}$ and $\tilde{\mu}_{ij}$ represent the reduced dielectric and magnetic permeability coefficients, respectively. These reduced material parameters are described as

$$\tilde{c}_{11}=c_{11}-\frac{c_{13}^2}{c_{33}},\quad \tilde{c}_{44}=c_{44},\quad \tilde{e}_{31}=e_{31}-\frac{c_{13}e_{33}}{c_{33}},\quad \tilde{e}_{15}=e_{15},\quad \tilde{q}_{31}=q_{31}-\frac{c_{13}q_{33}}{c_{33}}, \tag{3.4a}$$
$$\tilde{s}_{11}=s_{11},\quad \tilde{s}_{33}=s_{33}+\frac{e_{33}^2}{c_{33}},\quad \tilde{d}_{11}=d_{11},\quad \tilde{d}_{33}=d_{33}+\frac{q_{33}e_{33}}{c_{33}},\quad \tilde{\mu}_{11}=\mu_{11}, \tag{3.4b}$$
$$\tilde{\mu}_{33}=\mu_{33}+\frac{q_{33}^2}{c_{33}},\quad \tilde{q}_{15}=q_{15},\quad \tilde{\beta}_1=\beta_1-\frac{c_{13}\beta_3}{c_{33}},\quad \tilde{p}_3=p_3+\frac{\beta_3 e_{33}}{c_{33}},\quad \tilde{\lambda}_3=\lambda_3+\frac{\beta_3 q_{33}}{c_{33}}. \tag{3.4c}$$

Moreover, E_i and H_i denote the electric and magnetic fields intensity, respectively. Utilizing the quasi-static approximation, the electric and magnetic fields intensity can be obtained as

$$\mathbf{E}=-\nabla\Phi, \tag{3.5a}$$
$$\mathbf{H}=-\nabla\Psi, \tag{3.5b}$$

where Φ and Ψ denote the scalar electric and magnetic potentials, respectively. Moreover, it is approximately assumed that the distributions of electric and magnetic potentials are as follows

$$\Phi=-\cos(\beta z)\phi_E(t,x)+\frac{2z}{h}V_E, \tag{3.6a}$$
$$\Psi=-\cos(\beta z)\psi_H(t,x)+\frac{2z}{h}\Omega_H, \tag{3.6b}$$

in which $\beta=\pi/h$, V_E and Ω_H are the initial applied electric voltage and magnetic potential, respectively. Also, Φ_E and Ψ_H represent the spatial variation of the electric and magnetic potentials in the x-directions, respectively.

$$E_x=-\frac{\partial\Phi}{\partial x}=\cos(\beta z)\frac{\partial\phi_E}{\partial x},\qquad E_z=-\frac{\partial\Phi}{\partial z}=-\beta\sin(\beta z)\phi_E-\frac{2V_E}{h}, \tag{3.7a}$$
$$H_x=-\frac{\partial\Psi}{\partial x}=\cos(\beta z)\frac{\partial\psi_H}{\partial x},\qquad H_z=-\frac{\partial\Psi}{\partial z}=-\beta\sin(\beta z)\psi_H-\frac{2\Omega_H}{h}. \tag{3.7b}$$

The strain energy of the first-order shear deformable piezoelectric-piezomagnetic nanobeams can be expressed as

$$\begin{aligned}\Pi_{s1}=&\frac{1}{2}\int_0^L\int_A(\sigma_{xx}\varepsilon_{xx}+\sigma_{xz}\gamma_{xz}-D_xE_x-D_zE_z-B_xH_x-B_zH_z)\,dA\,dx\\ =&\frac{1}{2}\int_0^L\left\{N_x\left[\frac{\partial U}{\partial x}+\frac{1}{2}\left(\frac{\partial W}{\partial x}\right)^2\right]+M_x\frac{\partial\Theta_x}{\partial x}+Q_x\left(\frac{\partial W}{\partial x}+\Theta_x\right)\right\}dx\\ &+\frac{1}{2}\int_0^L\int_A\left(-D_x\cos(\beta z)\frac{\partial\phi_E}{\partial x}+D_z\left(\beta\sin(\beta z)\phi_E+\frac{2V_E}{h}\right)\right)dA\,dx\\ &+\frac{1}{2}\int_0^L\int_A\left(-B_x\cos(\beta z)\frac{\partial\psi_H}{\partial x}+B_z\left(\beta\sin(\beta z)\psi_H+\frac{2\Omega_H}{h}\right)\right)dA\,dx,\end{aligned}\tag{3.8}$$

where the normal resultant force N_x, shear force Q_x and bending moment M_x in a section are expressed as

$$N_x=\int_A\sigma_{xx}dA,\quad M_x=\int_A\sigma_{xx}z\,dA,\quad Q_x=\kappa_s\int_A\sigma_{xz}dA,\tag{3.9}$$

in which κ_s is the shear correction factor. Moreover, the kinetic energy of piezoelectric-piezomagnetic nanobeam; Π_T can be described as follows:

$$\begin{aligned}\Pi_T=&\frac{1}{2}\int_0^L\int_A\rho\left\{\left(\frac{\partial u_x}{\partial t}\right)^2+\left(\frac{\partial u_z}{\partial t}\right)^2\right\}dA\,dx\\ =&\frac{1}{2}\int_0^L\left[I_0\left(\frac{\partial U}{\partial t}\right)^2+I_2\left(\frac{\partial\Theta_x}{\partial t}\right)^2+I_1\left(\frac{\partial W}{\partial t}\right)^2\right]dx,\end{aligned}\tag{3.10}$$

where $\{I_0,I_2\}=\rho\{A,I\}$ and $A=bh$, $I=(bh^3)/12$.

The Hamilton principle is employed to derive the geometrically nonlinear governing equations of motion of first-order shear deformable piezoelectric-piezomagnetic nanobeams and associated with corresponding boundary conditions. Thus, the geometrically nonlinear governing equations are obtained as

$$\frac{\partial N_x}{\partial x}=I_0\frac{\partial^2U}{\partial t^2},\tag{3.11a}$$

$$\frac{\partial}{\partial x}\left(N_x\frac{\partial W}{\partial x}\right)+\frac{\partial Q_x}{\partial x}=I_0\frac{\partial^2W}{\partial t^2},\tag{3.11b}$$

$$\frac{\partial M_x}{\partial x}-Q_x=I_2\frac{\partial^2\Theta_x}{\partial t^2},\tag{3.11c}$$

$$\int_A\left(\cos(\beta z)\frac{\partial D_x}{\partial x}+\beta\sin(\beta z)D_z\right)dA=0,\tag{3.11d}$$

$$\int_A\left(\cos(\beta z)\frac{\partial B_x}{\partial x}+\beta\sin(\beta z)B_z\right)dA=0.\tag{3.11e}$$

Moreover, the corresponding essential and natural boundary conditions can be expressed as

$$\delta U=0 \quad \text{or} \quad N_x=0, \tag{3.12a}$$

$$\delta W=0 \quad \text{or} \quad N_x\frac{\partial W}{\partial x}+Q_x=0, \tag{3.12b}$$

$$\delta\Theta_x=0 \quad \text{or} \quad M_x=0, \tag{3.12c}$$

$$\phi_E=0 \quad \text{or} \quad \int_A \cos(\beta z)D_x dA=0, \tag{3.12d}$$

$$\delta\psi_H=0 \quad \text{or} \quad \int_A \cos(\beta z)B_x dA=0. \tag{3.12e}$$

The aforementioned governing equations are derived according to the classical shear deformable theory. Therefore, they are not capable of depicting the small-scale effect due to the lack of a material length scale parameter. Hence, the nonlocal elasticity theory is used to incorporate the material length scale parameter into account. According to the Eqs. (2.1), (3.2), (3.7) and (3.9), one can write the following nonlocal relations in a section of the piezoelectric-piezomagnetic nanobeams

$$N_x-(e_0a)^2\frac{\partial^2 N_x}{\partial x^2}=A_{11}\left[\frac{\partial U}{\partial x}+\frac{1}{2}\left(\frac{\partial W}{\partial x}\right)^2\right]+N_E+N_H+N_T, \tag{3.13a}$$

$$M_x-(e_0a)^2\frac{\partial^2 M_x}{\partial x^2}=D_{11}\frac{\partial\Theta_x}{\partial x}+E_{31}\phi_E+Q_{31}\psi_H, \tag{3.13b}$$

$$Q_x-(e_0a)^2\frac{\partial^2 Q_x}{\partial x^2}=k_sA_{44}\left(\Theta_x+\frac{\partial W}{\partial x}\right)-\kappa_sE_{15}\frac{\partial\phi_E}{\partial x}-\kappa_sQ_{15}\frac{\partial\psi_H}{\partial x}, \tag{3.13c}$$

$$\int_A\left\{D_x-(e_0a)^2\frac{\partial^2 D_x}{\partial x^2}\right\}\cos(\beta z)dA=E_{15}\left(\Theta_x+\frac{\partial W}{\partial x}\right)+X_{11}\frac{\partial\phi_E}{\partial x}+Y_{11}\frac{\partial\psi_H}{\partial x}, \tag{3.13d}$$

$$\int_A\left\{D_z-(e_0a)^2\frac{\partial^2 D_z}{\partial x^2}\right\}\beta\sin(\beta z)dA=E_{31}\frac{\partial\Theta_x}{\partial x}-X_{33}\phi_E-Y_{33}\psi_H, \tag{3.13e}$$

$$\int_A\left\{B_x-(e_0a)^2\frac{\partial^2 B_x}{\partial x^2}\right\}\cos(\beta z)dA=Q_{15}\left(\Theta_x+\frac{\partial W}{\partial x}\right)+Y_{11}\frac{\partial\phi_E}{\partial x}+T_{11}\frac{\partial\psi_H}{\partial x}, \tag{3.13f}$$

$$\int_A\left\{B_z-(e_0a)^2\frac{\partial^2 B_z}{\partial x^2}\right\}\beta\sin(\beta z)dA=Q_{31}\frac{\partial\Theta_x}{\partial x}-Y_{33}\phi_E-T_{33}\psi_H, \tag{3.13g}$$

where

$$N_E=\frac{2\tilde{e}_{31}V_EA}{h},\quad N_H=\frac{2\tilde{q}_{31}\Omega_HA}{h},\quad N_T=-\tilde{\beta}_1A\Delta T, \tag{3.14a}$$

$$A_{11}=\tilde{c}_{11}A,\quad A_{44}=\tilde{c}_{44}A,\quad D_{11}=\tilde{c}_{11}I, \tag{3.14b}$$

$$E_{31}=\int_A\tilde{e}_{31}\beta\sin(\beta z)zdA,\quad Q_{31}=\int_A\tilde{q}_{31}\beta\sin(\beta z)zdA, \tag{3.14c}$$

$$E_{15}=\int_A\tilde{e}_{15}\cos(\beta z)dA,\quad Q_{15}=\int_A\tilde{q}_{15}\cos(\beta z)dA, \tag{3.14d}$$

$$X_{11}=\int_A \tilde{s}_{11}\cos^2(\beta z)dA,\quad Y_{11}=\int_A \tilde{d}_{11}\cos^2(\beta z)dA,\quad T_{11}=\int_A \tilde{\mu}_{11}\cos^2(\beta z)dA, \tag{3.14e}$$

$$X_{33}=\int_A \tilde{s}_{33}[\beta\sin(\beta z)]^2dA,\ Y_{33}=\int_A \tilde{d}_{33}[\beta\sin(\beta z)]^2dA,\ T_{33}=\int_A \tilde{\mu}_{33}[\beta\sin(\beta z)]^2dA. \tag{3.14f}$$

Using Eqs. (3.11a)-(3.11c) and (3.13a)-(3.13c), the explicit form of N_x, M_x and Q_x including the nonlocal parameter can be expressed as

$$N_x=A_{11}\left[\frac{\partial U}{\partial x}+\frac{1}{2}\left(\frac{\partial W}{\partial x}\right)^2\right]+N_E+N_H+N_T+(e_0a)^2I_0\frac{\partial^3 U}{\partial t^2\partial x}, \tag{3.15a}$$

$$M_x=D_{11}\frac{\partial\Theta_x}{\partial x}+E_{31}\phi_E+Q_{31}\psi_H+(e_0a)^2\left\{I_0\frac{\partial^2 W}{\partial t^2}+I_2\frac{\partial^3\Theta_x}{\partial t^2\partial x}-\frac{\partial}{\partial x}\left(N_x\frac{\partial W}{\partial x}\right)\right\}, \tag{3.15b}$$

$$Q_x=k_sA_{44}\left(\Theta_x+\frac{\partial W}{\partial x}\right)-\kappa_sE_{15}\frac{\partial\phi_E}{\partial x}-\kappa_sQ_{15}\frac{\partial\psi_H}{\partial x}+(e_0a)^2\frac{\partial}{\partial x}\left\{I_0\frac{\partial^2 W}{\partial t^2}-\frac{\partial}{\partial x}\left(N_x\frac{\partial W}{\partial x}\right)\right\}. \tag{3.15c}$$

Note that inserting Eqs. (3.13d) and (3.13e) into Eqs. (3.11d)-(3.13g) is unable to give the explicit forms of D_x, D_z, B_x and B_z. However, the size-dependent geometrically nonlinear governing equations for piezoelectric-piezomagnetic nanobeams in terms of displacement can be obtained by substituting Eq. (3.15) and other related equations into Eq. (3.11) and can be expressed as follows:

$$A_{11}\left(\frac{\partial^2 U}{\partial x^2}+\frac{\partial W}{\partial x}\frac{\partial^2 W}{\partial x^2}\right)=I_0\left[\frac{\partial^2 U}{\partial t^2}-(e_0a)^2\frac{\partial^4 U}{\partial t^2\partial x^2}\right], \tag{3.16a}$$

$$\begin{aligned}&k_sA_{44}\left(\frac{\partial\Theta_x}{\partial x}+\frac{\partial^2 W}{\partial x^2}\right)+(N_E+N_H+N_T)\left(\frac{\partial^2 W}{\partial x^2}-(e_0a)^2\frac{\partial^4 W}{\partial x^4}\right)\\&-\kappa_s\left(E_{15}\frac{\partial^2\phi_E}{\partial x^2}+Q_{15}\frac{\partial^2\psi_H}{\partial x^2}\right)+Z_1-(e_0a)^2Z_2=I_0\left(\frac{\partial^2 W}{\partial t^2}-(e_0a)^2\frac{\partial^4 W}{\partial t^2\partial x^2}\right),\end{aligned} \tag{3.16b}$$

$$\begin{aligned}&D_{11}\frac{\partial^2\Theta_x}{\partial x^2}-k_sA_{44}\left(\Theta_x+\frac{\partial W}{\partial x}\right)+(E_{31}+\kappa_sE_{15})\frac{\partial\phi_E}{\partial x}+(Q_{31}+\kappa_sQ_{15})\frac{\partial\phi_E}{\partial x}\\&=I_2\left(\frac{\partial^2\Theta_x}{\partial t^2}-(e_0a)^2\frac{\partial^4\Theta_x}{\partial t^2\partial x^2}\right),\end{aligned} \tag{3.16c}$$

$$E_{31}\frac{\partial\Theta_x}{\partial x}+E_{15}\left(\frac{\partial^2 W}{\partial x^2}+\frac{\partial\Theta_x}{\partial x}\right)+X_{11}\frac{\partial^2\phi_E}{\partial x^2}+Y_{11}\frac{\partial^2\psi_H}{\partial x^2}-X_{33}\phi_E-Y_{33}\psi_H=0, \tag{3.16d}$$

$$Q_{31}\frac{\partial\Theta_x}{\partial x}+Q_{15}\left(\frac{\partial^2 W}{\partial x^2}+\frac{\partial\Theta_x}{\partial x}\right)+Y_{11}\frac{\partial^2\phi_E}{\partial x^2}+T_{11}\frac{\partial^2\psi_H}{\partial x^2}-Y_{33}\phi_E-T_{33}\psi_H=0, \tag{3.16e}$$

where

$$Z_1=A_{11}\left(\frac{\partial^2 U}{\partial x^2}\frac{\partial W}{\partial x}+\frac{\partial U}{\partial x}\frac{\partial^2 W}{\partial x^2}+\frac{3}{2}\left(\frac{\partial W}{\partial x}\right)^2\frac{\partial^2 W}{\partial x^2}\right), \tag{3.17a}$$

$$Z_2=A_{11}\left(\frac{\partial^4 U}{\partial x^4}\frac{\partial W}{\partial x}+3\frac{\partial^3 U}{\partial x^3}\frac{\partial^2 W}{\partial x^2}+3\frac{\partial^2 U}{\partial x^2}\frac{\partial^3 W}{\partial x^3}+\frac{\partial U}{\partial x}\frac{\partial^4 W}{\partial x^4}\right)$$

$$+A_{11}\left[3\left(\frac{\partial^2 W}{\partial x^2}\right)^2+9\frac{\partial W}{\partial x}\frac{\partial^2 W}{\partial x^2}\frac{\partial^3 W}{\partial x^3}+\frac{3}{2}\left(\frac{\partial W}{\partial x}\right)^2\frac{\partial^4 W}{\partial x^4}\right]. \tag{3.17b}$$

Introducing the following non-dimensional quantities

$$\xi=\frac{x}{L},\quad (u,w)=\frac{(U,W)}{h},\quad \theta_x=\Theta_x,\quad \phi=\frac{\phi_E}{\phi_0},\quad \psi=\frac{\psi_H}{\psi_0},\quad \phi_0=\sqrt{A_{11}/X_{33}}, \tag{3.18a}$$

$$\psi_0=\sqrt{A_{11}/T_{33}},\quad \tau=\frac{t}{L}\sqrt{A_{11}/I_0},\quad \varepsilon=\frac{e_0 a}{L},\quad \eta=\frac{L}{h},\quad (\bar{N}_T,\bar{N}_E,\bar{N}_H)=\left(\frac{N_T}{A_{11}},\frac{N_E}{A_{11}},\frac{N_H}{A_{11}}\right), \tag{3.18b}$$

$$(\bar{A}_{11},\bar{A}_{44},\bar{D}_{11})=\left(\frac{A_{11}}{A_{11}},\frac{A_{44}}{A_{11}},\frac{D_{11}}{A_{11}h^2}\right),\quad (\bar{I}_0,\bar{I}_2)=\left(\frac{I_0}{I_0},\frac{I_2}{I_0h^2}\right),\quad (\bar{E}_{15},\bar{E}_{31})=\left(\frac{E_{15}\phi_0}{A_{11}h},\frac{E_{31}\phi_0}{A_{11}h}\right), \tag{3.18c}$$

$$(\bar{Q}_{15},\bar{Q}_{31})=\left(\frac{Q_{15}\psi_0}{A_{11}h},\frac{Q_{31}\psi_0}{A_{11}h}\right),\quad (\bar{X}_{11},\bar{X}_{33})=\left(\frac{X_{11}\phi_0^2}{A_{11}h^2},\frac{X_{33}\phi_0^2}{A_{11}}\right), \tag{3.18d}$$

$$(\bar{T}_{11},\bar{T}_{33})=\left(\frac{T_{11}\psi_0^2}{A_{11}h^2},\frac{T_{33}\psi_0^2}{A_{11}}\right),\quad (\bar{Y}_{11},\bar{Y}_{33})=\left(\frac{Y_{11}\phi_0\psi_0}{A_{11}h^2},\frac{Y_{33}\phi_0\psi_0}{A_{11}}\right), \tag{3.18e}$$

the non-dimensional form of size-dependent geometrically nonlinear governing equations (3.13) can be expressed as

$$\bar{A}_{11}\left(\frac{\partial^2 u}{\partial\xi^2}+\frac{1}{\eta}\frac{\partial w}{\partial\xi}\frac{\partial^2 w}{\partial\xi^2}\right)=\bar{I}_0\left(\frac{\partial^2 u}{\partial\tau^2}-{}^2\frac{\partial^4 u}{\partial\tau^2\partial\xi^2}\right), \tag{3.19a}$$

$$k_s\bar{A}_{44}\left(\frac{\partial^2 w}{\partial\xi^2}+\eta\frac{\partial\theta_x}{\partial\xi}\right)+(\bar{N}_T+\bar{N}_E+\bar{N}_H)\left(\frac{\partial^2 w}{\partial\xi^2}-{}^2\frac{\partial^4 w}{\partial\xi^4}\right)-k_s\bar{E}_{15}\frac{\partial^2\bar{\phi}_E}{\partial\xi^2}-k_s\bar{Q}_{15}\frac{\partial^2\bar{\psi}_H}{\partial\xi^2}+\bar{Z}_1$$
$$-{}^2\bar{Z}_2=\bar{I}_0\left(\frac{\partial^2 w}{\partial\tau^2}-{}^2\frac{\partial^4 w}{\partial\tau^2\partial\xi^2}\right), \tag{3.19b}$$

$$\bar{D}_{11}\frac{\partial^2\theta_x}{\partial\xi^2}-k_s\bar{A}_{44}\eta\left(\frac{\partial w}{\partial\xi}+\eta\theta_x\right)+\eta(\bar{E}_{31}+\kappa_s\bar{E}_{15})\frac{\partial\phi}{\partial\xi}+\eta\left(\bar{Q}_{31}+\kappa_s\bar{Q}_{15}\right)\frac{\partial\psi}{\partial\xi}$$
$$=\bar{I}_2\left(\frac{\partial^2\theta_x}{\partial\tau^2}-{}^2\frac{\partial^4\theta_x}{\partial\tau^2\partial\xi^2}\right), \tag{3.19c}$$

$$\bar{E}_{31}\eta\frac{\partial\theta_x}{\partial\xi}+\bar{E}_{15}\left(\frac{\partial^2 w}{\partial\xi^2}+\eta\frac{\partial\theta_x}{\partial\xi}\right)+\bar{X}_{11}\frac{\partial^2\phi}{\partial\xi^2}+\bar{Y}_{11}\frac{\partial^2\psi}{\partial\xi^2}-\bar{X}_{33}\eta^2\phi-\bar{Y}_{33}\eta^2\psi=0, \tag{3.19d}$$

$$\bar{Q}_{31}\eta\frac{\partial\theta_x}{\partial\xi}+Q_{15}\left(\frac{\partial^2 w}{\partial\xi^2}+\eta\frac{\partial\theta_x}{\partial\xi}\right)+\bar{Y}_{11}\frac{\partial^2\phi}{\partial\xi^2}+\bar{T}_{11}\frac{\partial^2\psi}{\partial\xi^2}-\bar{Y}_{33}\eta^2\phi-\bar{T}_{33}\eta^2\psi=0, \tag{3.19e}$$

where

$$\bar{Z}_1=\frac{a_{11}}{\eta}\left(\frac{\partial^2 u}{\partial\xi^2}\frac{\partial w}{\partial\xi}+\frac{1}{\eta}\left(\frac{\partial w}{\partial\xi}\right)^2\frac{\partial^2 w}{\partial\xi^2}+\frac{\partial u}{\partial\xi}\frac{\partial^2 w}{\partial\xi^2}\right), \tag{3.20a}$$

$$\bar{Z}_2=\frac{a_{11}}{\eta}\left(\frac{\partial^4 u}{\partial\xi^4}\frac{\partial w}{\partial\xi}+3\frac{\partial^3 u}{\partial\xi^3}\frac{\partial^2 w}{\partial\xi^2}+3\frac{\partial^2 u}{\partial\xi^2}\frac{\partial^3 w}{\partial\xi^3}+\frac{\partial u}{\partial\xi}\frac{\partial^4 w}{\partial\xi^4}\right)$$

$$+\frac{a_{11}}{\eta^2}\left[3\left(\frac{\partial^2 w}{\partial\xi^2}\right)^3+9\frac{\partial w}{\partial\xi}\frac{\partial^2 w}{\partial\xi^2}\frac{\partial^3 w}{\partial\xi^3}+\frac{3}{2}\left(\frac{\partial w}{\partial\xi}\right)^2\frac{\partial^4 w}{\partial\xi^4}\right]. \tag{3.20b}$$

The electric potential and magnetic potential can be assumed to be zero at the two ends of the piezoelectric-piezomagnetic nanobeams. Therefore, the following boundary conditions can be considered for the piezoelectric-piezomagnetic nanobeams under various types of edge supports

$$u=w=\theta_x=\phi=\psi=0 \quad \text{at } \xi=0,1, \tag{3.21}$$

for a clamped-clamped (C-C) edge supports,

$$u=w=\bar{M}_x=\phi=\psi=0 \quad \text{at } \xi=0,1, \tag{3.22}$$

for a simply supported -simply supported (SS-SS) edge supports and

$$u=w=\theta_x=\phi=\psi=0 \qquad \text{at } \xi=0, \tag{3.23a}$$

$$u=w=\bar{M}_x=\phi=\psi=0 \qquad \text{at } \xi=1, \tag{3.23b}$$

for a clamped -simply supported (C-SS) edge supports, in which

$$\begin{aligned}\bar{\mathrm{M}}_{\mathrm{x}}=&\bar{D}_{11}\frac{\partial\theta_x}{\partial\xi}+\eta\bar{E}_{31}\phi+\eta\bar{Q}_{31}\psi+\epsilon^2\left(\bar{I}_0\eta\frac{\partial^2 w}{\partial\tau^2}+\bar{I}_2\frac{\partial^3\psi}{\partial\tau^2\partial\xi}-\eta\left(\bar{N}_E+\bar{N}_H+\bar{N}_T\right)\frac{\partial^2 w}{\partial\xi^2}\right)\\&-\epsilon^2\bar{A}_{11}\frac{\partial}{\partial\xi}\left(\left[\frac{\partial u}{\partial\xi}+\frac{1}{2\eta}\left(\frac{\partial w}{\partial\xi}\right)^2\right]\frac{\partial w}{\partial\xi}\right).\end{aligned} \tag{3.24}$$

4 Numerical solution approach

In this section, an efficient numerical solution approach is utilized to solve the problem of the geometrically nonlinear free vibration of piezoelectric-piezomagnetic nanobeams. To this end, the GDQ method [52–54] as a high accurate and convergent strategy is utilized to discretize the nonlinear equations of motion and associated boundary conditions in the spatial domain. Afterwards, the numerical Galerkin method is applied to the aforementioned discretized equations to obtain a set of Duffing-type ordinary differential equations. Then, the periodic time differential operators are introduced to achieve a set of nonlinear algebraic parameterized equations. Finally, the set of nonlinear algebraic equations is solved by means of the pseudo arc-length continuation algorithm to calculate nonlinear frequency-response of piezoelectric-piezomagnetic nanobeams.

4.1 Discretization

Based upon the shifted ChebyshevGaussLobatto grid points, the discrete grid points in ξ_i direction can be generated as

$$\xi_i=\frac{1}{2}\left(1-\cos\frac{i-1}{N-1}\pi\right), \quad i=1,2,\cdots,N, \tag{4.1}$$

in which N is the number of total grid points in ξ-direction. Therefore, the discretized form of displacement components u, w, θ_x, the electric potential ϕ and magnetic potential ψ can be expressed as follows:

$$\mathbf{U}=\begin{bmatrix} u_1 & u_2 & \cdots & u_N \end{bmatrix}^{\mathrm{T}},\ \mathbf{W}=\begin{bmatrix} w_1 & w_2 & \cdots & w_N \end{bmatrix}^{\mathrm{T}},\ \theta=\begin{bmatrix} \theta_{x1} & \theta_{x2} & \cdots & \theta_{xN} \end{bmatrix}^{\mathrm{T}}, \tag{4.2a}$$

$$\mathbf{\Phi}=\begin{bmatrix} \phi_1 & \phi_2 & \cdots & \phi_N \end{bmatrix}^{\mathrm{T}},\ \mathbf{\Psi}=\begin{bmatrix} \psi_1 & \psi_2 & \cdots & \psi_N \end{bmatrix}^{\mathrm{T}}, \tag{4.2b}$$

in which $u_i=u(\xi_i)$, $w_i=w(\xi_i)$, $\theta_{xi}=\theta_x(\xi_i)$, $\phi_i=\phi(\xi_i)$ and $\psi_i=\psi(\xi_i)$. The discretized governing equations of motion can be written in a matrix form as

$$\mathbf{M}\ddot{\mathbf{X}}+\mathbf{K}\mathbf{X}+\mathbf{N}(\mathbf{X})=0, \tag{4.3}$$

in which field variables vector $\mathbf{X}$, stiffness matrix $\mathbf{K}$, mass matrix $\mathbf{M}$ and nonlinear part vector $\mathbf{N}(\mathbf{X})$ are defined as

$$\mathbf{X}=\begin{bmatrix} \mathbf{U}^{\mathrm{T}} & \mathbf{W}^{\mathrm{T}} & \boldsymbol{\theta}^{\mathrm{T}} & \mathbf{\Phi}^{\mathrm{T}} & \boldsymbol{\psi}^{\mathrm{T}} \end{bmatrix}^{\mathrm{T}}, \tag{4.4a}$$

$$\mathbf{K}=\begin{bmatrix} \bar{A}_{11}\mathbf{D}_{\xi}^{(2)} & \mathbf{0} & \mathbf{0} & \mathbf{0} & \mathbf{0} \\ \mathbf{0} & k_s\bar{A}_{44}\mathbf{D}_{\xi}^{(2)}+N_0^x & k_s\bar{A}_{44}\eta\mathbf{D}_{\xi}^{(1)} & -k_s\bar{E}_{15}\mathbf{D}_{\xi}^{(2)} & \mathbf{0} \\ \mathbf{0} & -k_s\bar{A}_{44}\mathbf{D}\eta_{\xi}^{(1)} & -k_s\bar{A}_{44}\eta^2\mathbf{D}_{\xi}^{(0)}+\bar{D}_{11}\mathbf{D}_{\xi}^{(2)} & -k_s\bar{A}_{44}\eta^2\mathbf{D}_{\xi}^{(0)}+\bar{D}_{11}\mathbf{D}_{\xi}^{(2)} & \mathbf{0} \\ \mathbf{0} & \bar{\mathrm{E}}_{15}\mathbf{D}_{\xi}^{(2)} & (\bar{E}_{31}+\bar{\mathrm{E}}_{15})\eta\mathbf{D}_{\xi}^{(1)} & -\bar{X}_{33}\eta^2\mathbf{D}_{\xi}^{(0)}+\bar{X}_{11}\mathbf{D}_{\xi}^{(2)} & \mathbf{0} \\ \mathbf{0} & \bar{\mathrm{Q}}_{15}\mathbf{D}_{\xi}^{(2)} & \left(\bar{Q}_{31}+\bar{\mathrm{Q}}_{15}\right)\eta\mathbf{D}_{\xi}^{(1)} & -\bar{Y}_{33}\eta^2\mathbf{D}_{\xi}^{(0)}+\bar{Y}_{11}\mathbf{D}_{\xi}^{(2)} & \mathbf{0} \\ \mathbf{0} & -k_s\bar{\mathrm{Q}}_{15}\mathbf{D}_{\xi}^{(2)} & \eta\left(\bar{Q}_{31}+\kappa_s\bar{\mathrm{Q}}_{15}\right)\mathbf{D}_{\xi}^{(1)} & -\bar{Y}_{33}\eta^2\mathbf{D}_{\xi}^{(0)}+\bar{Y}_{11}\mathbf{D}_{\xi}^{(2)} & -\bar{T}_{33}\eta^2\mathbf{D}_{\xi}^{(0)}+\bar{T}_{11}\mathbf{D}_{\xi}^{(2)} \end{bmatrix}, \tag{4.4b}$$

$$\mathbf{M}=-\begin{bmatrix} \bar{I}_0\left(\mathbf{D}_{\xi}^{(0)}-{}^2\mathbf{D}_{\xi}^{(2)}\right) & 0 & 0 & 0 & 0 \\ 0 & \bar{I}_0\left(\mathbf{D}_{\xi}^{(0)}-{}^2\mathbf{D}_{\xi}^{(2)}\right) & 0 & 0 & 0 \\ 0 & 0 & \bar{I}_2\left(\mathbf{D}_{\xi}^{(0)}-{}^2\mathbf{D}_{\xi}^{(2)}\right) & 0 & 0 \\ 0 & 0 & 0 & 0 & 0 \\ 0 & 0 & 0 & 0 & 0 \end{bmatrix}, \tag{4.4c}$$

$$\mathbf{N}(\mathbf{X})=\begin{bmatrix} \mathbf{N}_u^{\mathrm{T}}(\mathbf{X}) & \mathbf{N}_w^{\mathrm{T}}(\mathbf{X}) & \mathbf{N}_\theta^{\mathrm{T}}(\mathbf{X}) & \mathbf{N}_\phi^{\mathrm{T}}(\mathbf{X}) & \mathbf{N}_\psi^{\mathrm{T}}(\mathbf{X}) \end{bmatrix}^{\mathrm{T}}, \tag{4.4d}$$

where

$$N_0^x=(\bar{N}_T+\bar{N}_E+\bar{N}_H)\left(\mathbf{D}_{\xi}^{(2)}-{}^2\mathbf{D}_{\xi}^{(4)}\right).$$

Moreover, the components of $\mathbf{N}(\mathbf{X})$ can be expressed as

$$\mathbf{N}_u(\mathbf{X}) = \frac{\bar{A}_{11}}{\eta}\left(\mathbf{D}_\xi^{(1)}\mathbf{W}\right)\circ\left(\mathbf{D}_\xi^{(2)}\mathbf{W}\right), \tag{4.5a}$$

$$\begin{aligned}&\mathbf{N}_w(\mathbf{X})\\&= \frac{\bar{A}_{11}}{\eta}\left(\left(\mathbf{D}_\xi^{(1)}\mathbf{U}\right)\circ\left(\mathbf{D}_\xi^{(2)}\mathbf{W}\right)+\left(\mathbf{D}_\xi^{(2)}\mathbf{U}\right)\circ\left(\mathbf{D}_\xi^{(3)}\mathbf{W}\right)+\frac{3}{2\eta}\left(\mathbf{D}_\xi^{(2)}\mathbf{W}\right)\circ\left(\mathbf{D}_\xi^{(1)}\mathbf{W}\right)\circ\left(\mathbf{D}_\xi^{(1)}\mathbf{W}\right)\right)\\&\quad-\epsilon^2\left\{\frac{\bar{A}_{11}}{\eta}\left(\left(\mathbf{D}_\xi^{(4)}\mathbf{U}\right)\circ\left(\mathbf{D}_\xi^{(1)}\mathbf{W}\right)+3\left(\mathbf{D}_\xi^{(3)}\mathbf{U}\right)\circ\left(\mathbf{D}_\xi^{(2)}\mathbf{W}\right)+3\left(\mathbf{D}_\xi^{(2)}\mathbf{U}\right)\circ\left(\mathbf{D}_\xi^{(3)}\mathbf{W}\right)+\left(\mathbf{D}_\xi^{(1)}\mathbf{U}\right)\circ\left(\mathbf{D}_\xi^{(4)}\mathbf{W}\right)\right)\right.\\&\quad\left.+\frac{\bar{A}_{11}}{\eta^2}\left(3\left(\mathbf{D}_\xi^{(2)}\mathbf{W}\right)\circ\left(\mathbf{D}_\xi^{(2)}\mathbf{W}\right)\circ\left(\mathbf{D}_\xi^{(2)}\mathbf{W}\right)+9\left(\mathbf{D}_\xi^{(1)}\mathbf{W}\right)\circ\left(\mathbf{D}_\xi^{(2)}\mathbf{W}\right)\circ\left(\mathbf{D}_\xi^{(3)}\mathbf{W}\right)+\frac{3}{2}\left(\mathbf{D}_\xi^{(1)}\mathbf{W}\right)\circ\left(\mathbf{D}_\xi^{(1)}\mathbf{W}\right)\circ\left(\mathbf{D}_\xi^{(4)}\mathbf{W}\right)\right)\right\},\end{aligned} \tag{4.5b}$$

$$\mathbf{N}_\theta(\mathbf{X}) = \mathbf{N}_\phi(\mathbf{X}) = \mathbf{N}_\psi(\mathbf{X}) = 0, \tag{4.5c}$$

in which $\circ$ denotes the Hadamard product (see the Appendix). Moreover, the weighting coefficients corresponding to the r-th-order derivative with respect to ξ can be calculated by means of the following equation

$$\left[\mathbf{D}_\xi^{(r)}\right]_{ij} = \mathcal{W}_{ij}^{(r)} = \begin{cases}\mathbf{I}_x, & r=0,\\ \dfrac{\mathcal{P}(\xi_i)}{\left(\xi_i-\xi_j\right)\mathcal{P}\left(\xi_j\right)}, & i\neq j \text{ and } i,j=1,\cdots,N \text{ and } r=1,\\ r\left[\mathcal{W}_{ij}^{(1)}\mathcal{W}_{ii}^{(r-1)}-\dfrac{\mathcal{W}_{ij}^{(r-1)}}{\xi_i-\xi_j}\right], & i\neq j \text{ and } i,j=1,\cdots,N \text{ and } r=2,3,\cdots,N-1,\\ -\sum\limits_{j=1;\ j\neq i}^{N}\mathcal{W}_{ij}^{(r)}, & i=j \text{ and } i,j=1,\cdots,N \text{ and } r=1,2,3,\cdots,N-1,\end{cases} \tag{4.6}$$

where $\mathbf{I}_x$ stands for a $N\times N$ identity matrix and

$$\mathcal{P}(x_i) = \prod_{j=1;\ j\neq i}^{N}\left(\xi_i-\xi_j\right).$$

The boundary conditions can be discretized in a same way. For instance, the discretized counterpart of Eq. (3.11) corresponding to the nanobeams with C-C end support is given by

$$\mathbf{U}=\mathbf{W}=\boldsymbol{\theta}=\boldsymbol{\Phi}=\boldsymbol{\psi}=0 \quad \text{at } \xi=0,1. \tag{4.7}$$

4.2 Duffing-type equations

A numerical Galerkin technique is utilized to covert the discretized nonlinear Eq. (4.3) into a time-varying set of Duffing-type ordinary differential equations. Hence, neglecting the nonlinear term in Eq. (4.3) and considering the harmonic solution as

$$\mathbf{X} = \tilde{\mathbf{X}}e^{j\omega_l\tau}$$

result in the following eigenvalue problem

$$\mathbf{K}\tilde{\mathbf{X}} = -\omega_l^2\mathbf{M}\tilde{\mathbf{X}}, \tag{4.8}$$

in which ω_l denotes the linear frequency of piezoelectric-piezomagnetic nanobeams. After replacing the discretized boundary conditions elements associated with the boundary nodes in the aforementioned matrices and solving the obtained eigenvalue problem, the calculated linear mode shapes can be expressed as follows:

$$\mathbf{X}=\mathbf{\Phi q}, \tag{4.9}$$

in which $\mathbf{q}$ is the reduced generalized coordinates. Also, $\mathbf{\Phi}$ stands for a sparse matrix including the first m eigenvectors which is utilized as the base function in the numerical Galerkin technique. $\mathbf{q}$ and $\mathbf{\Phi}$ are defined as follows

$$\begin{aligned}\mathbf{q}^{\mathrm{T}}{}_{(5m)\times 1}=\Big[\ & q_u^1 \quad q_u^2 \quad \cdots \quad q_u^m \quad q_w^1 \quad q_w^2 \quad \cdots \quad q_w^m \quad q_\theta^1 \quad q_\theta^2 \quad \cdots \quad q_\theta^m \quad q_\phi^1 \quad q_\phi^2 \quad \cdots \\ & q_\phi^m \quad q_\psi^1 \quad q_\psi^2 \quad \cdots \quad q_\psi^m \ \Big],\end{aligned} \tag{4.10a}$$

$$\mathbf{\Phi}_{(5N)\times(5m)}=\begin{bmatrix}\mathbf{\Phi}_u & 0 & 0 & 0\\ 0 & \mathbf{\Phi}_w & 0 & 0\\ 0 & 0 & \mathbf{\Phi}_\psi & 0\\ 0 & 0 & 0 & \mathbf{\Phi}_\varphi\end{bmatrix} \tag{4.10b}$$

with

$$\mathbf{\Phi}_{uN\times m}=\Big[\ \big[\tilde{\mathbf{X}}_u^1\big]_{N\times 1} \quad \cdots \quad \big[\tilde{\mathbf{X}}_u^m\big]_{N\times 1}\ \Big], \tag{4.11a}$$

$$\mathbf{\Phi}_{wN\times m}=\Big[\ \big[\tilde{\mathbf{X}}_w^1\big]_{N\times 1} \quad \cdots \quad \big[\tilde{\mathbf{X}}_w^m\big]_{N\times 1}\ \Big], \tag{4.11b}$$

$$\mathbf{\Phi}_{\theta N\times m}=\Big[\ \big[\tilde{\mathbf{X}}_\theta^1\big]_{N\times 1} \quad \cdots \quad \big[\tilde{\mathbf{X}}_\theta^m\big]_{N\times 1}\ \Big], \tag{4.11c}$$

$$\mathbf{\Phi}_{\phi N\times m}=\Big[\ \Big[\tilde{\mathbf{X}}_\phi^1\Big]_{N\times 1} \quad \cdots \quad \Big[\tilde{\mathbf{X}}_\phi^m\Big]_{N\times 1}\ \Big], \tag{4.11d}$$

$$\mathbf{\Phi}_{\psi N\times m}=\Big[\ \Big[\tilde{\mathbf{X}}_\psi^1\Big]_{N\times 1} \quad \cdots \quad \Big[\tilde{\mathbf{X}}_\psi^m\Big]_{N\times 1}\ \Big]. \tag{4.11e}$$

Inserting Eq. (4.9) into the nonlinear set of discretized equation (4.3) gives the following residual vector

$$\mathbf{R}=\mathbf{M\Phi\ddot{q}}+\mathbf{K\Phi q}+\mathbf{K}_{nl}(\mathbf{\Phi q}). \tag{4.12}$$

Now, multiplying each equation by the associated linear mode shape and integrating along the piezoelectric-piezomagnetic nanobeam length, results in the following Duffing-type equation

$$\tilde{\mathbf{M}}\ddot{\mathbf{q}}+\tilde{\mathbf{K}}\mathbf{q}+\tilde{\mathbf{K}}_{nl}(\mathbf{q})=0, \tag{4.13}$$

in which

$$\mathbf{G}_{m\times 5N}=\mathbf{\Phi}^{\mathrm{T}}diag(\mathbf{S}),\quad \mathbf{S}=\Big[\ \mathbf{S}_\xi \quad \mathbf{S}_\xi \quad \mathbf{S}_\xi \quad \mathbf{S}_\xi \quad \mathbf{S}_\xi\ \Big]_{1\times(5N)}, \tag{4.14a}$$

$$\tilde{\mathbf{M}}=\mathbf{GM\Phi},\quad \tilde{\mathbf{K}}=\mathbf{GK\Phi},\quad \tilde{\mathbf{K}}_{nl}(\mathbf{q})=\mathbf{GK}_{nl}(\mathbf{\Phi q}). \tag{4.14b}$$

In the aforementioned equation, $\mathbf{S}_{\tilde{\xi}}$ denotes the integral operator (see the Appendix). Therefore, by utilizing the numerical Galerkin method, the $5N$ general coordinates are reduced to $5m$ reduced coordinates in which m denotes the number of selected mode shapes. Another benefits of present numerical Galerkin technique are that this method can be easily applied to all kinds of edge supports in addition to the essential boundary condition, the natural boundary conditions can be satisfied and also the nonlocal effect is incorporated into the mode shapes. Therefore, the desire accuracy can be obtained by lower numbers of mode shapes and significantly lower computational efforts.

4.3 Solution procedure in the time domain

Introducing $\tau^*=\tau/T$ and $\Omega=2\pi/T$, Eq. (4.13) can be expressed as

$$\left(\frac{\Omega}{2\pi}\right)^2\tilde{\mathbf{M}}\ddot{\mathbf{q}}+\tilde{\mathbf{K}}\mathbf{q}+\tilde{\mathbf{K}}_{nl}(\mathbf{q})=0. \tag{4.15}$$

To discretize Eq. (4.15) on the time domain, the discrete grid points in the time domain τ^* can be generated as

$$\tau_i^*=\frac{i}{N_t},\quad 0<\tau_i^*\leq 1,\quad i=1,2,\cdots,N_t=2k, \tag{4.16}$$

in which N_t stands for the number of discrete points on the time domain and must be an even number. Therefore, the discretized form associated with $\mathbf{q}$ in Eq. (4.10a) on the time domain can be expressed as follows

$$\begin{aligned}\mathbf{Q}_{5m\times N_t}=\Big[\ &\mathbf{q}^1_{u\,1\times N_t}\ \cdots\ \mathbf{q}^m_{u\,1\times N_t}\ \ \mathbf{q}^1_{w1\times N_t}\ \cdots\ \mathbf{q}^m_{w1\times N_t}\ \ \mathbf{q}^1_{\theta 1\times N_t}\ \cdots\ \mathbf{q}^m_{\theta\,1\times N_t}\\ &\mathbf{q}^1_{\phi 1\times N_t}\ \cdots\ \mathbf{q}^m_{\phi\,1\times N_t}\ \ \mathbf{q}^1_{\psi 1\times N_t}\ \cdots\ \mathbf{q}^m_{\psi\,1\times N_t}\ \Big].\end{aligned} \tag{4.17}$$

Now, the highly precise differentiation matrix operators which are calculated from the derivatives of periodic sinc function as base function in the spectral collocation method [55] are utilized to discretize the periodic problem (4.15) on the time domain. By means of Eqs. (4.15) and (4.17), one can write

$$\left(\frac{\Omega}{2\pi}\right)^2\tilde{\mathbf{M}}\mathbf{Q}\mathbf{D}_{\tau^{(2)^{\mathrm{T}}}}+\tilde{\mathbf{K}}\mathbf{Q}+\tilde{\mathbf{K}}_{nl}(\mathbf{Q})=0, \tag{4.18}$$

in which $\mathbf{D}_{\tau}^{(\,)}$ denotes the time differentiation matrix operator whose explicit formulation is defined as

$$\begin{cases} b_{11}=-\dfrac{{N_t}^2}{12}-\dfrac{1}{6}, \\ b_{i1}=\dfrac{(-1)^{i-1}}{2\sin^2\frac{\pi(i-1)}{N_t}}, \\ b_{1j}=\dfrac{(-1)^{N_t-j+1}}{2\sin^2\frac{\pi(N_t-j+1)}{N_t}}, \\ b_{(i+1)(j+1)}=b_{ij}, \end{cases} \quad i,j=2,3,4,\cdots,N_t, \quad \mathbf{D}_{\tau}^{(2)}=(2\pi)^2\left[b_{ij}\right], \tag{4.19}$$

in which $\mathbf{D}_{\tau}^{(2)}$ is Teoplitz matrix.

Considering the relation $(B^T\otimes A)vec(X)=vec(AXB)$ in which **A** and **B** represent the constant matrices, **X** denotes an unknown matrix, $vec(\mathbf{X})$ is the vectorization of matrix **X** and $\otimes$ stands for the Kronecker product (see the Appendix), the vectorized form of Eq. (4.18) can be expressed as

$$\left(\left(\frac{\Omega}{2\pi}\right)^2\left(\mathbf{D}_{\tau}^{(2)}\otimes\tilde{\mathbf{M}}\right)+\left(\mathbf{I}_{\tau}\otimes\tilde{\mathbf{K}}\right)\right)vec(\mathbf{Q})+vec\left(\tilde{\mathbf{K}}_{nl}(\mathbf{Q})\right)=0. \tag{4.20}$$

The preceding equation can be stated as the following set of nonlinear parameterized equations

$$\mathbf{H}:{}^{5m\times N_t+1}\rightarrow{}^{5m\times N_t}, \quad \mathbf{H}(vec(\mathbf{Q}),\Omega)=0, \tag{4.21}$$

that can be directly solved using the pseudo-arc length continuation technique [56] to obtained the nonlinear frequency-response of the piezoelectric-piezomagnetic nanobeams.

5 Results and discussion

On the basis of the proposed nonlocal nonlinear piezoelectric-piezomagnetic nanobeam model, the selected numerical results are presented on the size-dependent geometrically nonlinear free vibration of first-order shear deformable piezoelectric-piezomagnetic nanobeams with SS-SS, C-SS and C-C boundary conditions subjected to thermo-electromagnetic loadings. It is assumed that the nanobeam is made of the two-phase $BiTiO_3$-$CoFe_2O_4$ composites with the material properties given in Table 1 [45, 57–59]. The influences of the non-dimensional nonlocal parameter, temperature rise, initial applied voltage, initial applied magnetic potential and length-to-thickness ratio on the geometrically nonlinear free vibration characteristics of the first-order shear deformable piezoelectric-piezomagnetic nanobeams are discussed in detail.

Table 1: Material properties of $BiTiO_3CoFe_2O_4$ composite materials [57–59].

Properties	$BiTiO_3CoFe_2O_4$
Elastic (GPa)	$c_{11}=226$; $c_{12}=125$; $c_{13}=124$; $c_{33}=216$; $c_{44}=44.2$
Piezoelectric (C/m^2)	$e_{31}=2.2$; $e_{33}=9.3$; $e_{15}=5.8$
Dielectric ($10^9 C/V\cdot m$)	$s_{11}=5.64$; $s_{33}=6.35$
Piezomagnetic ($N/A\cdot m$)	$q_{15}=275$; $q_{31}=290.1$; $q_{33}=349.9$
Magnetoelectric ($10^{12} Ns/VC$)	$d_{11=5.367}$; $d_{33}=2737.5$
Magnetic ($10^6 Ns^2/C^2$)	$\mu_{11}=-297$; $\mu_{33}=83.5$
Thermal moduli ($10^5 N/K\cdot m^2$)	$\beta_1=4.74$; $\beta_3=4.53$
Pyroelectric ($10^6 C/N$)	$p_3=25$
Pyromagnetic ($10^6 N/A\cdot m\cdot K$)	$\lambda_3=5.19$
Mass density ($10^3 Kg/m^3$)	$\rho=5.55$

Table 2: Nonlinear frequency ratios for the isotropic homogeneous beams with C-C and SS-SS edge supports $(L/h=100)$.

$W_{\max}/r$	C-C		SS-SS	
	Present	Reference [60]	Present	Reference [60]
1	1.0297	1.0301	1.1178	1.1193
2	1.1145	1.1150	1.4171	1.4176
3	1.2418	1.2422	1.7892	1.8088
4	1.3979	1.3988	2.2394	2.2448
5	1.5746	1.5756	2.6873	2.6996

To check the accuracy of solution procedure for presented nonlinear analysis, the comparison of nonlinear frequency ratios (ω_{nl}/ω_l) corresponding to various nondimensional maximum vibration amplitude $(W_{\max}/r)$ for isotropic homogeneous beams with C-C and SS-SS edge supports obtained via the present solution and the direct iterative method given by Wu et al. [60] is provided in Table 2. Herein, $W_{\max}$ and $r=\sqrt{(I/A)}$ denote the maximum vibration amplitude and radius of gyration of the beam (I and A stand for the area moment of inertia and cross section area of beam with the rectangular cross-section). Excellent agreement is reached between the present results and those given by Wu et al. [60], that shows the validation of the present solution methodology. Furthermore, in order to verify the convergence of the present mathematical formulation, numerical method and also check the validity and accuracy of the present analysis, the first three natural frequencies of a piezoelectric-piezomagnetic nanobeam with different boundary conditions related to various total numbers of grid points are provided and are compared with those of the natural frequencies given in [45], as shown in Table 3. A reasonable agreement between the present results and those of [45] is observed. Moreover, according to Table 3, $N=15$ is used for all of the following numerical calculations.

In the following figures, the frequency ratio (ω_{Nl}/ω_l) versus the maximum vibration amplitude of piezoelectric-piezomagnetic nanobeam $(w_{\max})$ is plotted. The nonlinear and linear frequencies are denoted by ω_{Nl} and ω_l, respectively. The non-dimensional

Table 3: First three natural frequencies (GHz) of piezoelectric-piezomagnetic nanobeam with $\Delta T=0^{\circ}$C, $V_E=0$V, $\Omega_H=0$A, $\mu=0.1$.

Number of grid nodes	C-C			C-SS			SS-SS		
	ω_1	ω_2	ω_3	ω_1	ω_2	ω_3	ω_1	ω_2	ω_3
7	7.1228	15.6993	23.9546	5.1811	13.4399	21.9255	3.4945	11.3427	19.5048
9	7.1247	15.3315	22.9946	5.1822	13.4177	21.4648	3.4932	11.4073	19.8141
11	7.1246	15.3291	22.9849	5.1821	13.4098	21.4166	3.4932	11.4012	19.7389
13	7.1246	15.3290	22.9837	5.1820	13.4101	21.4191	3.4932	11.4013	19.7438
15	7.1246	15.3290	22.9838	5.1820	13.4101	21.4189	3.4932	11.4013	19.7436
17	7.1246	15.3290	22.9838	5.1820	13.4101	21.4189	3.4932	11.4013	19.7436
21	7.1246	15.3290	22.9838	5.1820	13.4101	21.4189	3.4932	11.4013	19.7436
25	7.1246	15.3290	22.9838	5.1820	13.4101	21.4189	3.4932	11.4013	19.7436
31	7.1246	15.3290	22.9838	5.1820	13.4101	21.4189	3.4932	11.4013	19.7436
Reference [45]	7.2371	15.615	23.4883	5.2781	13.6863	21.9225	3.5670	11.6620	20.2435

maximum amplitude is expressed as the ratio of the maximum amplitude to the thickness of the piezoelectric-piezomagnetic nanobeam (i.e., $w_{\max}=W_{\max}/h$) and the frequency ratio is described as the ratio of the nonlinear frequency to the linear frequency of the piezoelectric-piezomagnetic nanobeam. Moreover, the linear frequencies are given for a direct comparison.

Represented in Fig. 1 is the effect of the non-dimensional nonlocal parameter μ on the frequency-response of piezoelectric-piezomagnetic nanobeams with SS-SS, C-SS and C-C edge supports. In these figures, the nonlinear frequency curves associated with the classical piezoelectric-piezomagnetic beam model $(\mu=0)$ are given for a direct comparison. The vibrating piezoelectric-piezomagnetic nanobeams exhibit a hardening spring type of nonlinearity and the hardening behavior is seen at large amplitude, i.e., for all types of boundary conditions, the increase of the vibration amplitude causes the increase of the frequency ratio. The non-dimensional nonlocal parameter has a considerable effect on the geometrically nonlinear free vibration characteristics. For all types of edge supports and at a given vibration amplitude, the increase of non-dimensional nonlocal parameter leads to the decrease of non-dimensional linear and nonlinear frequencies and the increase of the frequency ratio and the hardening behavior of nanobeams. Moreover, the non-dimensional nonlocal parameter has more considerable effect on the hardening behavior of C-C piezoelectric-piezomagnetic nanobeams, while a weak effect on the SS-SS nanobeams is observed. It shows the necessity of such a size-dependent beam model for the analysis of geometrically nonlinear free vibration of the piezoelectric-piezomagnetic nanobeams, especially for nanobeams with C-C end supports.

The effect of the temperature rise on the frequency-response of piezoelectric-piezomagnetic nanobeams is illustrated in Fig. 2 . Due to the introducing the compressive in-plane forces, an increase in the temperature change decreases the linear frequency of piezoelectric-piezomagnetic nanobeams and causes the increase of the hardening behavior of nanobeams. However, the increase of the temperature change has not a considerable effect on the linear frequency and frequency ratio of nanobeams.

The effect of initial applied negative and positive electric voltages on the frequency response of piezoelectric-piezomagnetic nanobeams with different edge supports is in-

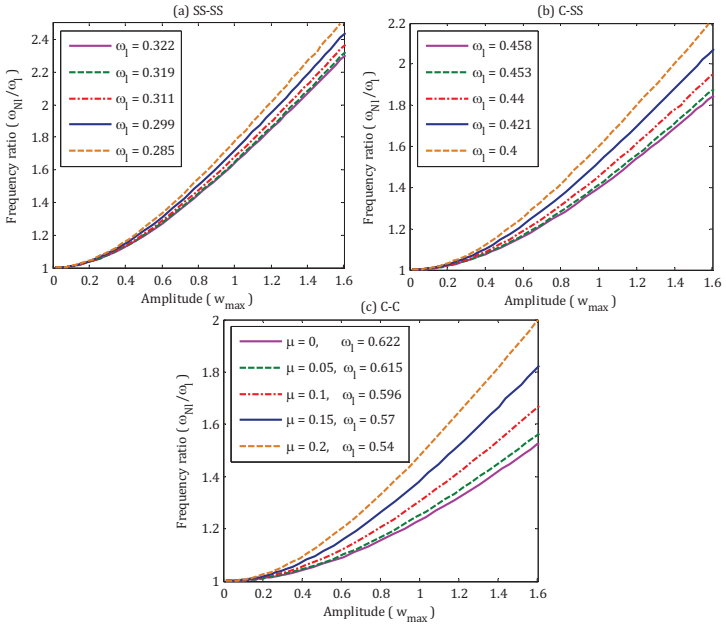

Figure 1: Frequencyresponse of piezoelectric-piezomagnetic nanobeams associated with different nonlocal parameters and boundary conditions ($L/h=10$, $h=10$nm, $V_E=-0.02$V, $\Omega_H=0.02$A, $\Delta T=20^\circ$C).

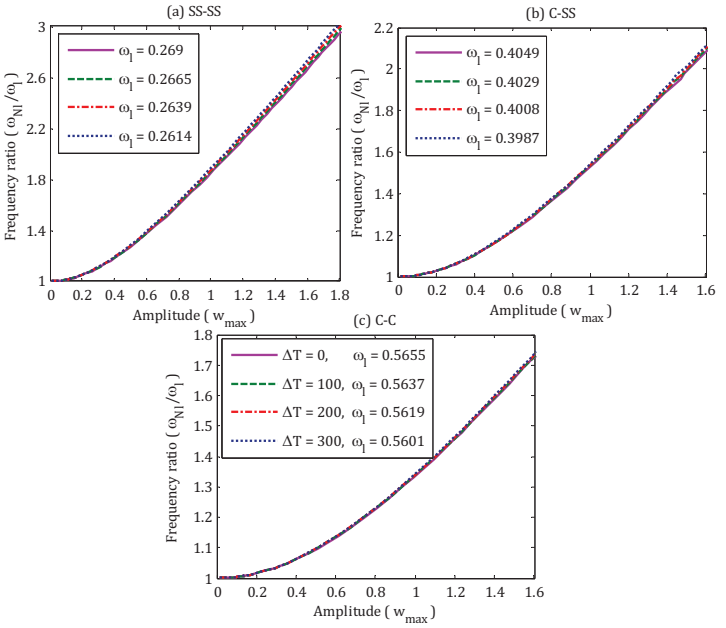

Figure 2: Frequencyresponse of piezoelectric-piezomagnetic nanobeams associated with different temperature changes and boundary conditions ($L/h=10$, $h=10$nm, $V_E=0$V, $\Omega_H=0$A, $\mu=0.1$).

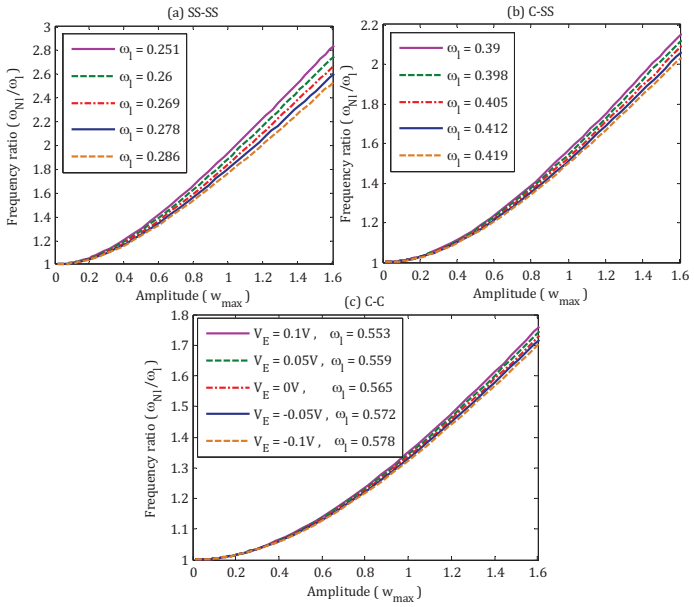

Figure 3: Frequencyresponse of piezoelectric-piezomagnetic nanobeams associated with different initial applied electric voltages and boundary conditions ($L/h=10$, $h=10$nm, $\Omega_H=0$A, $\Delta T=0^\circ$C, $\mu=0.1$).

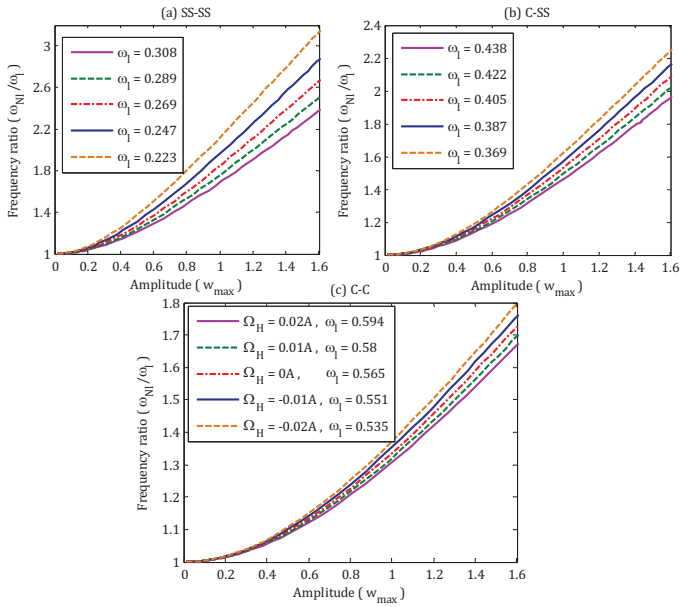

Figure 4: Frequencyresponse of piezoelectric-piezomagnetic nanobeams associated with different initial applied magnetic potentials and boundary conditions ($L/h=10$, $h=10$nm, $V_E=0$V, $\Delta T=0^\circ$C, $\mu=0.1$).

vestigated in Fig. 3 . Compared to the temperature change, it is seen that initial applied electric voltage has a considerable influence on the linear frequency, nonlinear frequency and typical hardening behavior of piezoelectric-piezomagnetic nanobeams. Because of the producing the compressive and tensile in-plane forces, respectively, the increase of the initial imposed positive and negative electric voltages decreases and increases the linear frequencies of nanobeams. Moreover, increasing the positive and negative electric voltages leads to a signicant increase and decrease in the typical hardening behaviors of nanobeams, respectively. This change is more considerable for piezoelectric-piezomagnetic nanobeams with SS-SS boundary conditions.

The effect of the initial applied magnetic potential on the frequency-response of piezoelectric-piezomagnetic nanobeams is also demonstrated in Fig. 4 . Both the linear and nonlinear frequencies of piezoelectric nanobeams decrease with increasing the negative initial applied magnetic potential. It is because that negative magnetic potential generates a compressive in-plane force in the nanobeams. Moreover, due to the introducing the tensile in-plane force, the stiffness of piezoelectric-piezomagnetic nanobeams increases as the positive magnetic potential increases. Therefore, the linear frequency increases and a decrease in the typical hardening behavior of nanobeams is observed, especially for the nanobeams with SS-SS edge supports.

The effect of length-to-thickness ratio (L/h) on the frequency-response of

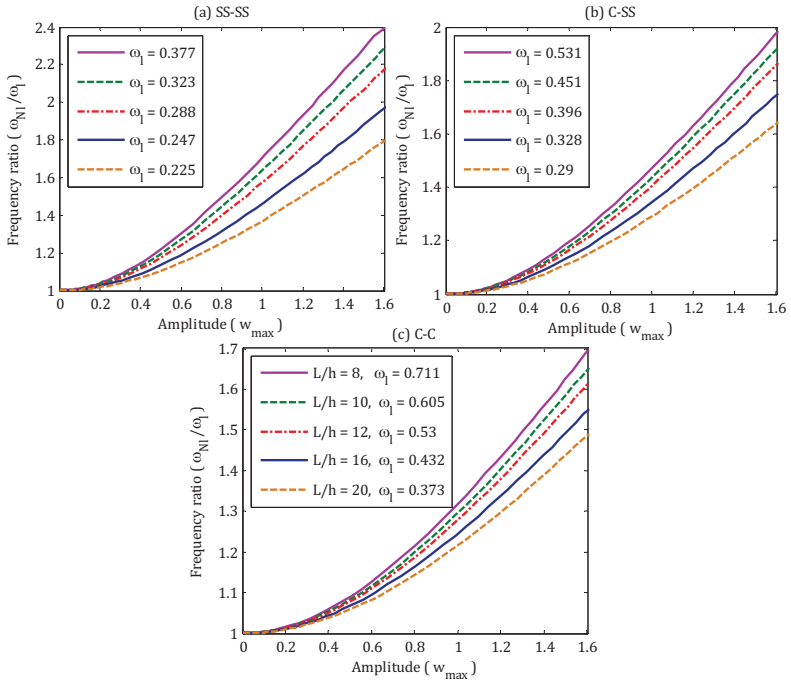

Figure 5: Frequencyresponse of piezoelectric-piezomagnetic nanobeams associated with length-to-thickness ratios and boundary conditions ($h=10$nm, $V_E=-0.1$V, $\Omega_H=0.02$A, $\Delta T=20^\circ$C, $\mu=0.1$).

piezoelectric-piezomagnetic nanobeams with various edge supports is studied in Fig. 5 . For all types of boundary conditions, the increase of the length-to-thickness ratio causes a decrease in both linear and nonlinear frequencies of the piezoelectric-piezomagnetic nanobeams. Moreover, the typical hardening behavior of nanobeams decreases as the length-to-thickness ratio increases.

6 Conclusions

The geometrically nonlinear free vibration of piezoelectric-piezomagnetic nanobeams under the magnetic, electric and thermal loadings was investigated by means of a proposed nonlocal rst-order shear deformable beam model. To this end, utilizing the first-order shear deformation theory and nonlocal elasticity theory, the nonlocal governing differential equations of motion and corresponding boundary conditions were derived with considering the influences of size effect, shear deformations, rotary inertia, piezoelectric-piezomagnetic coupling, thermal environment and geometrical nonlinearity. Then, the GDQ method was used to discretize the set of nonlinear PDEs. Next, the discretized PDEs were transformed to the Dufng-type ODEs by means of the numerical Galerkin method. The periodic time differential operators and pseudo arc-length continuation method were employed to numerically solve the set of nonlinear algebraic parameterized equations. Finally, the influences of the non-dimensional nonlocal parameter, temperature change, initial applied electric voltage, initial applied magnetic potential, length-to-thickness ratio and various boundary conditions on the geometrically nonlinear free vibration characteristics of piezoelectric-piezomagnetic nanobeams were investigated. The main results can be given as:

1. The non-dimensional nonlocal parameter reduces the natural frequencies, but increases the nonlinear frequency ratios of the piezoelectric-piezomagnetic nanobeams. In other words, the classical models overestimate and underestimate the natural frequencies and nonlinear frequency ratios, respectively.

2. The hardening spring effect increases with increasing the non-dimensional nonlocal parameter and decreases with increasing the length-to-thickness ratio, which indicates the necessity of implementing a nonlinear analysis in lower length-to-thickness ratios.

3. The natural frequencies of piezoelectric-piezomagnetic nanobeams decreases as the change in the temperature increases, but this change in the temperature has less significant effects on the nonlinear frequency ratio.

4. The positive and negative initial applied voltages decrease and increase the natural frequencies of piezoelectric-piezomagnetic nanobeams, respectively. Also, greater hardening effect is observed for the positive initial applied voltages.

5. A change in the initial applied magnetic potential from a positive value to a negative value decreases the natural frequencies and increases the nonlinear frequency ratio.

6. Greater hardening effect is observed for SS-SS piezoelectric-piezomagnetic nanobeams as compared to nanobeams with C-SS and C-C edge conditions.

Appendix

A Hadamard and Kronecker products

Definition A.1. Considering the matrices $\mathbf{A}=\left[A_{ij}\right]_{N\times M}$ and $\mathbf{B}=\left[B_{ij}\right]_{N\times M}$, the Hadamard product of these matrices can be stated as $\mathbf{A}\circ\mathbf{B}=\left[A_{ij}B_{ij}\right]_{N\times M}$.

Definition A.2. If $\mathbf{A}$ and $\mathbf{B}$ are m-by-n and p-by-q matrices, then the Kronecker product $\mathbf{A}\otimes\mathbf{B}$ denotes an mp-by-nq block matrix and defined as

$$\mathbf{A}\otimes\mathbf{B}=\begin{bmatrix} a_{11}\mathbf{B} & \cdots & a_{1n}\mathbf{B} \\ \vdots & \ddots & \vdots \\ a_{m1}\mathbf{B} & \cdots & a_{mn}\mathbf{B} \end{bmatrix}_{mp\times nq}.$$

B Integral matrix operators

$$\int_{x_1}^{x_N} f(x)dx=\left(\sum_{r=0}^{N-1}\tilde{\mathbf{X}}^{(r)}\mathbf{D}_x^{(r)}\right)\mathbf{F}=\mathbf{S}_x\mathbf{F},\mathbf{S}_x=[S_x]_{1\times N},$$

where $\mathbf{D}_x^{(r)}$ is the GDQ differential operator and

$$\tilde{\mathbf{X}}^{(r)}=\left[\frac{(x_2-x_1)^{r+1}}{2^{r+1}(r+1)!},\cdots,\frac{(x_{i+1}-x_i)^{r+1}-(x_{i-1}-x_i)^{r+1}}{2^{r+1}(r+1)!},\cdots,-\frac{(x_{N-1}-x_N)^{r+1}}{2^{r+1}(r+1)!}\right],$$
$$i=2,3,\cdots,N-1.$$

References

[1] J. VAN DEN BOOMGAARD, D. TERRELL, R. BORN AND H. GILLER, *An in situ grown eutectic magnetoelectric composite material,* J. Materials Sci., 9 (1974), pp. 1705–1709.

[2] Z. LANG AND L. XUEWU, *Buckling and vibration analysis of functionally graded magneto-electro-thermo-elastic circular cylindrical shells,* Appl. Math. Model., 37 (2013), pp. 2279–2292.

[3] S. BRISCHETTO AND E. CARRERA, *Coupled thermo-electro-mechanical analysis of smart plates embedding composite and piezoelectric layers,* J. Thermal Stresses, 35 (2012), pp. 766–804.

[4] A. BALLATO, *Modeling piezoelectric and piezomagnetic devices and structures via equivalent networks,* IEEE Transactions on Ultrasonics, Ferroelectrics and Frequency Control, 48 (2001), pp. 1189–1240.
[5] C. ZHANG, W. CHEN, J. LI AND J. YANG, *One-dimensional equations for piezoelectromagnetic beams and magnetoelectric effects in fibers,* Smart Materials Struct., 18 (2009), pp. 095026.
[6] C. WÖLFINGER, F. ARENDTS, K. FRIEDRICH AND K. DRECHSLER, *Health-monitoring-system based on piezoelectric transducers,* Aerospace Sci. Tech., 2 (1998), pp. 391–400.
[7] R. E. NEWNHAM, L. BOWEN, K. KLICKER AND L. CROSS, *Composite piezoelectric transducers,* Materials Design, 2 (1980), pp. 93–106.
[8] T. BAILEY AND J. UBBARD, *Distributed piezoelectric-polymer active vibration control of a cantilever beam,* J. Guidance, Control Dyn., 8 (1985), pp. 605–611.
[9] E. F. CRAWLEY AND J. DE LUIS, *Use of piezoelectric actuators as elements of intelligent structures,* AIAA J., 25 (1987), pp. 1373–1385.
[10] B. AZVINE, G. TOMLINSON AND R. WYNNE, *Use of active constrained-layer damping for controlling resonant vibration,* Smart Materials Struct., 4 (1995), pp. 1.
[11] A. BAZ, *Robust control of active constrained layer damping,* J. Sound Vib., 211 (1998), pp. 467–480.
[12] A. Q. JIANG, C. WANG, K. J. JIN, X. B. LIU, J. F. SCOTT, C. S. HWANG AND ET AL., *A resistive memory in semiconducting $BiFeO_3$ thin-film capacitors,* Adv. Materials, 23 (2011), pp. 1277–1281.
[13] N. A. FLECK, G. M. MULLER, M. F. ASHBY AND J. W. HUTCHINSON, *Strain gradient plasticity: theory and experiment,* Acta Metallurgica et Materialia, 42 (1994), pp. 475–487.
[14] J. S. STÖLKEN AND A. G. EVANS, *A microbend test method for measuring the plasticity length scale,* Acta Mater., 46 (1998), pp. 5109–5115.
[15] A. W. MCFARLAND AND J. S. COLTON, *Role of material microstructure in plate stiffness with relevance to microcantilever sensors,* J. Micromech. Microeng., 15 (2005), pp. 1060.
[16] W. D. NIX AND H. GAO, *Indentation size effects in crystalline materials: a law for strain gradient plasticity,* J. Mech. Phys. Solids, 46 (1998), pp. 411–425.
[17] S. CUENOT, C. FRÉTIGNY, S. DEMOUSTIER-CHAMPAGNE AND B. NYSTEN, *Surface tension effect on the mechanical properties of nanomaterials measured by atomic force microscopy,* Phys. Rev. B, 69 (2004), pp. 165410.
[18] E. W. WONG, P. E. SHEEHAN AND C. M. LIEBER, *Nanobeam mechanics: elasticity, strength and toughness of nanorods and nanotubes,* Science, 277 (1997), pp. 1971–1975.
[19] C. SUN AND H. ZHANG, *Size-dependent elastic moduli of platelike nanomaterials,* J. Appl. Phys., 93 (2003), pp. 1212–1218.
[20] H. ZHANG AND C. SUN, *Nanoplate model for platelike nanomaterials,* AIAA J., 42 (2004), pp. 2002–2009.
[21] J. PEDDIESON, G. R. BUCHANAN AND R. P. MCNITT, *Application of nonlocal continuum models to nanotechnology,* Int. J. Eng. Sci., 41 (2003), pp. 305–312.
[22] R. ANSARI, R. GHOLAMI AND S. AJORI, *Torsional vibration analysis of carbon nanotubes based on the strain gradient theory and molecular dynamic simulations,* J. Vib. Acoustics, 135 (2013), pp. 051016.
[23] A. C. ERINGEN, *Linear theory of nonlocal elasticity and dispersion of plane waves,* Int. J. Eng. Sci., 10 (1972), pp. 425–435.
[24] R. D. MINDLIN, *Micro-structure in linear elasticity,* Archive Rational Mech. Anal., 16 (1964), pp. 51–78.
[25] F. YANG, A. C. M. CHONG, D. C. C. LAM AND P. TONG, *Couple stress based strain gradient*

theory for elasticity, Int. J. Solids Struct., 39 (2002), pp. 2731–2743.
[26] D. C. C. LAM, F. YANG, A. C. M. CHONG, J. WANG AND P. TONG, *Experiments and theory in strain gradient elasticity,* J. Mech. Phys. Solids, 51 (2003), pp. 1477–1508.
[27] M. E. GURTIN AND A. I. MURDOCH, *A continuum theory of elastic material surfaces,* Archive Rational Mech. Anal., 57 (1975), pp. 291–323.
[28] M. E. GURTIN AND A. I. MURDOCH, *Surface stress in solids,* Int. J. Solids Struct., 14 (1978), pp. 431–440.
[29] R. ANSARI, H. RAMEZANNEZHAD AND R. GHOLAMI, *Nonlocal beam theory for nonlinear vibrations of embedded multiwalled carbon nanotubes in thermal environment,* Nonlinear Dyn., 67 (2012), pp. 2241–2254.
[30] R. ANSARI, R. GHOLAMI AND H. ROUHI, *Size-dependent nonlinear forced vibration analysis of magneto-electro-thermo-elastic Timoshenko nanobeams based upon the nonlocal elasticity theory,* Composite Struct., 126 (2015), pp. 216–226.
[31] J. REDDY, *Nonlocal nonlinear formulations for bending of classical and shear deformation theories of beams and plates,* Int. J. Eng. Sci., 48 (2010), pp. 1507–1518.
[32] R. GHOLAMI, R. ANSARI, A. DARVIZEH AND S. SAHMANI, *Axial buckling and dynamic stability of functionally graded microshells based on the modified couple stress theory,* Int. J. Struct. Stab. Dyn., 15 (2015), pp. 1450070.
[33] L.-L. KE, Y.-S. WANG, J. YANG AND S. KITIPORNCHAI, *Free vibration of size-dependent Mindlin microplates based on the modified couple stress theory,* J. Sound Vib., 331 (2012), pp. 94–106.
[34] R. ANSARI, R. GHOLAMI, M. FAGHIH SHOJAEI, V. MOHAMMADI AND M. DARABI, *Surface stress effect on the pull-in instability of hydrostatically and electrostatically actuated rectangular nanoplates with various edge supports,* J. Eng. Mater. Tech., 134 (2012), pp. 041013.
[35] M. R. NAMI, M. JANGHORBAN AND M. DAMADAM, *Thermal buckling analysis of functionally graded rectangular nanoplates based on nonlocal third-order shear deformation theory,* Aerospace Sci. Tech., 41 (2015), pp. 7–15.
[36] R. ANSARI AND R. GHOLAMI, *Size-dependent modeling of the free vibration characteristics of postbuckled third-order shear deformable rectangular nanoplates based on the surface stress elasticity theory,* Composites Part B Eng., 95 (2016), pp. 301–316.
[37] R. GHOLAMI, A. DARVIZEH, R. ANSARI AND F. SADEGHI, *Vibration and buckling of first-order shear deformable circular cylindrical micro-/nano-shells based on Mindlin's strain gradient elasticity theory,* Euro. J. Mech. A Solids, 58 (2016), pp. 76–88.
[38] L.-L. KE AND Y.-S. WANG, *Thermoelectric-mechanical vibration of piezoelectric nanobeams based on the nonlocal theory,* Smart Materials Struct., 21 (2012), pp. 025018.
[39] L.-L. KE, Y.-S. WANG AND Z.-D. WANG, *Nonlinear vibration of the piezoelectric nanobeams based on the nonlocal theory,* Composite Struct., 94 (2012), pp. 2038–2047.
[40] C. LIU, L.-L. KE, Y. WANG, J. YANG AND S. KITIPORNCHAI, *Buckling and post-buckling of size-dependent piezoelectric Timoshenko nanobeams subject to thermo-electro-mechanical loadings,* Int. J. Struct. Stability Dyn., 14 (2014), pp. 1350067.
[41] C. LIU, L.-L. KE, Y.-S. WANG, J. YANG AND S. KITIPORNCHAI, *Thermo-electro-mechanical vibration of piezoelectric nanoplates based on the nonlocal theory,* Composite Struct., 106 (2013), pp. 167–174.
[42] L.-L. KE, C. LIU AND Y.-S. WANG, *Free vibration of nonlocal piezoelectric nanoplates under various boundary conditions,* Physica E: Low-Dimensional Systems and Nanostructures, 66 (2015), pp. 93–106.
[43] S. ASEMI, A. FARAJPOUR AND M. MOHAMMADI, *Nonlinear vibration analysis of piezoelectric*

nanoelectromechanical resonators based on nonlocal elasticity theory, Composite Structures, 116 (2014), pp. 703–712.

[44] L. L. KE, Y. S. WANG AND J. N. REDDY, *Thermo-electro-mechanical vibration of size-dependent piezoelectric cylindrical nanoshells under various boundary conditions,* Composite Structures, 116 (2014), pp. 626–636.

[45] L.-L. KE AND Y.-S. WANG, *Free vibration of size-dependent magneto-electro-elastic nanobeams based on the nonlocal theory,* Physica E: Low-dimensional Systems and Nanostructures, 63 (2014), pp. 52–61.

[46] R. ANSARI AND R. GHOLAMI, *Nonlocal free vibration in the pre-and post-buckled states of magneto-electro-thermo elastic rectangular nanoplates with various edge conditions,* Smart Materials Struct., 25 (2016), pp. 095033.

[47] L.-L. KE, Y.-S. WANG, J. YANG AND S. KITIPORNCHAI, *Free vibration of size-dependent magneto-electro-elastic nanoplates based on the nonlocal theory,* Acta Mech. Sinica, 30 (2014), pp. 516–525.

[48] L.-L. KE, Y.-S. WANG, J. YANG AND S. KITIPORNCHAI, *The size-dependent vibration of embedded magneto-electro-elastic cylindrical nanoshells,* Smart Mater. Struct., 23 (2014), pp. 125036.

[49] A. C. ERINGEN, *Nonlocal polar elastic continua,* Int. J. Eng. Sci., 10 (1972), pp. 1–16.

[50] A. C. ERINGEN, *On differential equations of nonlocal elasticity and solutions of screw dislocation and surface waves,* J. Appl. Phys., 54 (1983), pp. 4703–4710.

[51] A. C. ERINGEN, Nonlocal Continuum Field Theories: Springer Science & Business Media, 2002.

[52] C. SHU, Differential Quadrature and Its Application in Engineering: Springer Science & Business Media, 2000.

[53] H. DU, M. LIM AND R. LIN, *Application of generalized differential quadrature method to structural problems,* Int. J. Numer. Methods Eng., 37 (1994), pp. 1881–1896.

[54] C. SHU AND H. DU, *A generalized approach for implementing general boundary conditions in the GDQ free vibration analysis of plates,* Int. J. Solids Structures, 34 (1997), pp. 837–846.

[55] L. N. TREFETHEN, *Spectral methods in MATLAB,* 10 (2000), Siam.

[56] H. B. KELLER, *Numerical solution of bifurcation and nonlinear eigenvalue problems,* Appl. Bifurcation Theory, (1977), pp. 359–384.

[57] J. Y. LI, *Magnetoelectroelastic multi-inclusion and inhomogeneity problems and their applications in composite materials,* Int. Eng. Sci., 38 (2000), pp. 1993–2011.

[58] W. BIN, Y. JIANGONG AND H. CUNFU, *Wave propagation in non-homogeneous magneto-electro-elastic plates*, J. Sound Vib., 317 (2008), pp. 250–264.

[59] P.-F. HOU, G.-H. TENG AND H.-R. CHEN, *Three-dimensional Green's function for a point heat source in two-phase transversely isotropic magneto-electro-thermo-elastic material,* Mech. Mater., 41 (2009), pp. 329–338.

[60] H. WU, J. YANG AND S. KITIPORNCHAI, *Nonlinear vibration of functionally graded carbon nanotube-reinforced composite beams with geometric imperfections,* Composites Part B Eng., 90 (2016), pp. 86–96.